Cellular and Molecular Bioengineering, Vol. 5, No. 2, June 2012 *(© 2012)* pp. 143–154
DOI: 10.1007/s12195-012-0225-z

BMES BIOMEDICAL ENGINEERING SOCIETY™ www.bmes.org

Coordinated Mechanosensitivity of Membrane Rafts and Focal Adhesions

DANIELA E. FUENTES and PETER J. BUTLER

Department of Bioengineering, The Pennsylvania State University, 205 Hallowell Building, University Park, PA 16802, USA

(Received 14 November 2011; accepted 16 February 2012; published online 24 February 2012)

Associate Editor David J. Odde oversaw the review of this article.

Abstract—Endothelial cells sense mechanical forces of blood flow through mechanisms that involve focal adhesions (FAs). The mechanosensitive pathways that originate from FA-associated integrin activation may involve membrane rafts, small cholesterol- and sphigolipid-rich domains that are either immobilized, by virtue of their attachment to the cytoskeleton, or highly mobile in the plane of the plasma membrane. In this study, we fluorescently labeled non-mobile and mobile populations of GM1, a ganglioside associated with lipid rafts, and transfected cells with the red fluorescent protein-(RFP-) talin, an indicator of integrin activation at FAs, in order to determine the kinetics and sequential order of raft and talin mechanosensitivity. Cells were imaged under confocal microscopy during mechanical manipulation of a FA induced by a fibronectin (FN)-functionalized nanoelectrode with feedback control of position. First, FA deformation led to long range deformation of immobile rafts followed by active recoil of a subpopulation of displaced rafts. Second, initial adhesion between the FN-probe and the cell induced rapid accumulation of GM1 at the probe site with a time constant of 1.7 s. Talin accumulated approximately 20 s later with a time constant of 0.6 s. Third, a 1 μm deformation of the FA lead to immediate (0.3 s) increase in GM1 fluorescence and a later (6 s) increase in talin. Fourth, long term deformation of FAs led to continual GM1 accumulation at the probe site that was reversed upon removal of the deformation. These results demonstrate that rafts are directly mechanosensitive and that raft mobility may enable the earliest events related to FA mechanosensing and reinforcement upon force application.

Keywords—Mechanotransduction, Endothelial cells, Membrane rafts, Focal adhesion, Scanning ion conductance microscopy, Talin.

INTRODUCTION

The cellular plasma membrane is a heterogeneous mixture of lipids that dynamically coalesces into domains according to lipid preferences for liquid-ordered and liquid-disordered phases. Membrane rafts are an important type of liquid-ordered domain that are highly transient, tens of nanometers in size, and enriched in cholesterol and sphingolipids.[56] Rafts dynamically combine and disperse to facilitate protein sequestration and protein–protein and protein–lipid interactions.[5,26,36,72] These domains, besides being rich in cholesterol, are associated with the ganglioside GM1, a glycosphingolipid that, when tagged with fluorescence, can be used as a marker of lipid rafts.[30,50,55] Membrane rafts may also play a role in cell mechanics[42,54] as they can modulate the clustering of integrins[9] which regulate cytoskeletal organization, membrane trafficking[23,60] and connections to the extracellular matrix[28,53] *via* focal adhesions (FAs). The association of cholesterol-rich domains and integrins and involvement of Rac and Rho[14–16,61] with membrane rafts suggests that rafts play a role in FA assembly and reinforcement, although this hypothesis has not yet been tested directly. Raft lipids may regulate protein localization and function through enhanced affinity between lipids and specific amino acid sequences in a protein's extracellular,[71] transmembrane,[58] or intracellular domains.[13] Such spatially and temporally regulated lipid–protein interaction that facilitates protein–raft association may permit the cell to regulate polarized sorting and signal transduction processes.

Rafts associate with integrins and may facilitate mechanosensation through integrin ligation and clustering, which are physiologically and clinically relevant to vascular tone regulation and shear-induced gene expression leading to atherogenesis. For example, Jalali *et al.*[37] showed that shear stress caused an increase in new ligand binding of β_1 integrins in and around FAs of endothelial cells (ECs) plated on fibronectin (FN) and an increase in ligand binding of β_3 integrins in ECs plated on vitronectin. In *ex vivo* arteriolar preparations, activation of the vitronectin receptor, $\alpha_v\beta_3$-integrin, and FN receptor, $\alpha_5\beta_1$-integrin, induced coronary arteriolar dilation by stimulating

Address correspondence to Peter J. Butler, Department of Bioengineering, The Pennsylvania State University, 205 Hallowell Building, University Park, PA 16802, USA. Electronic mail: pbutler@psu.edu

endothelial production of cyclooxygenase-derived prostaglandins[31] which dilate blood vessels.[6,21] Thus integrin–matrix interactions at FAs are required to initiate the signaling pathway leading to shear stress-induced vasodilation and blood pressure regulation. Integrins are associated with rafts and nucleate actin polymerization (reviewed in Levitan and Gooch[42]) by concentrating phophatidylinositol 4,5 biphosphate (PIP_2).[41] FAs are also cholesterol rich microdomains, and β_1 integrins are required for raft formation[16,61] and signaling through Rac-1.[16] Wang and colleagues found that Src-activation colocalized with Lyn, a raft marker[46] supporting an emerging picture of rafts as dynamic nanodomains that cluster the necessary critical mass of receptors[66] for downstream signaling through important mechanotransduction pathways, such as mitogen activated protein kinases (MAPK),[59] with time scales of formation of 20 ms and length scales of tens of nanometers.[18] Finally, EC membrane microdomains are themselves known to be differentially sensitive to fluid shear stress[65] making rafts a central focus of mechanosensation leading to vasoregulation and atherogenesis.

Despite the convergence of research on FA mechanosensing and lipid raft function, to date no studies have provided direct evidence for mechanical coupling between membrane rafts and FAs nor has the dynamic kinetic response of rafts to mechanical perturbation of FAs been elucidated. This study was undertaken to directly measure mechanical coupling between induced FAs and stable lipid rafts and to measure the kinetics of mobile raft coalescence at FAs upon FA formation and mechanical perturbation (Fig. 1). The study was enabled by a newly developed technique based on scanning ion conductance microscopy in which a FN-functionalized nanoelectrode was used to induce a FA and the precise timing of adhesion was determined through analysis of current through the electrode.[22] Subsequently, adhesion formation was followed by nanomechanical manipulation of the induced FA. Fluorescently labeled GM1 was used to assay raft dynamics and red fluorescent protein (RFP)-talin was used to assay FA formation and integrity, since talin binds to activated integrins through enhanced affinity between talin and integrin–integrin dimers.[1,2,4,7,8]

MATERIALS AND METHODS

Cell Culture and Fluorescence Labeling of Rafts and Talin

All *in vitro* experiments were performed on bovine aortic endothelial cells (BAECs) (VEC technologies, Rensselaer, NY) sub-cultured between passages 3–10 with MCDB-131 complete medium (VEC technologies, Rensselaer, NY) at 37 °C in a gas mixture of 95% air and 5% CO_2 with 90% humidity. Red fluorescent protein (RFP)-talin fusion plasmids (Invitrogen) were transfected into cells using BacMam technology (Invitrogen). The cells were then seeded onto chambered coverglasses or temperature-controlled chambers (Bioptechs, Butler, PA, USA) and placed in the incubator for 2 h, after which new MCDB-131 media was added. BAECs were incubated overnight prior to experiments. Membrane rafts were labeled by conjugating GM1 with Alexa Fluor 488-tagged recombinant cholera toxin-subunit B (CT-B) (Invitrogen) with the cells at 4 °C for 15 min, rinsed three times with DPBS, and followed by CT-B crosslinking with anti-cholera toxin subunit B antibody (anti–CT-B) (Invitrogen) at 4 °C for 10 min. Cells were slowly brought back to room temperature prior to experiments.

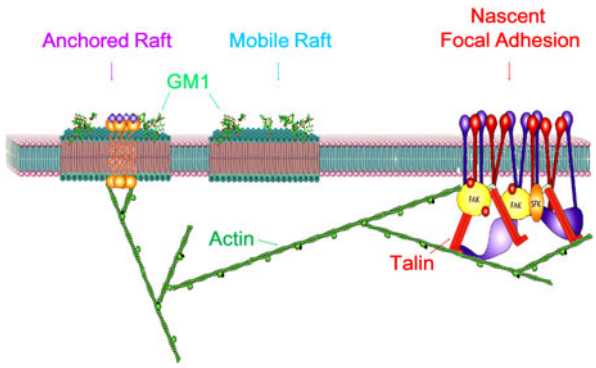

FIGURE 1. The membrane raft and FA connection: membrane rafts, rich in sphingolipids and cholesterol are identified by ganglioside marker GM1. Transmembrane proteins in some membrane rafts render a raft anchored *via* linkage to the cytoskeleton. In contrast, mobile rafts have no direct or indirect connection to the cytoskeleton. Focal adhesion sites, areas of clustered activated integrins linked to the cytoskeleton *via* talin, are known mechanotransducers. The connection between membrane rafts and FAs may involve both the cytoskeleton and the membrane.

Experimental Setup

A schematic representation of the experimental setup is shown in Fig. 2 and has been previously described.[17] Briefly, chambers containing cultured BAECs were placed on a piezoelectric stage (Nano-View & NanoDrive, Mad City Labs, Madison, WI, USA). An inverted Olympus IX71 microscope with a 100 W halogen light provided brightfield illumination for phase contrast. Fluorescence imaging was done with an oil-immersion objective (PlanAPO 60X/1.45 NA). Cellular fluorescence was assayed using a laser scanning confocal scanner system (VT-Infinity3, Visitech

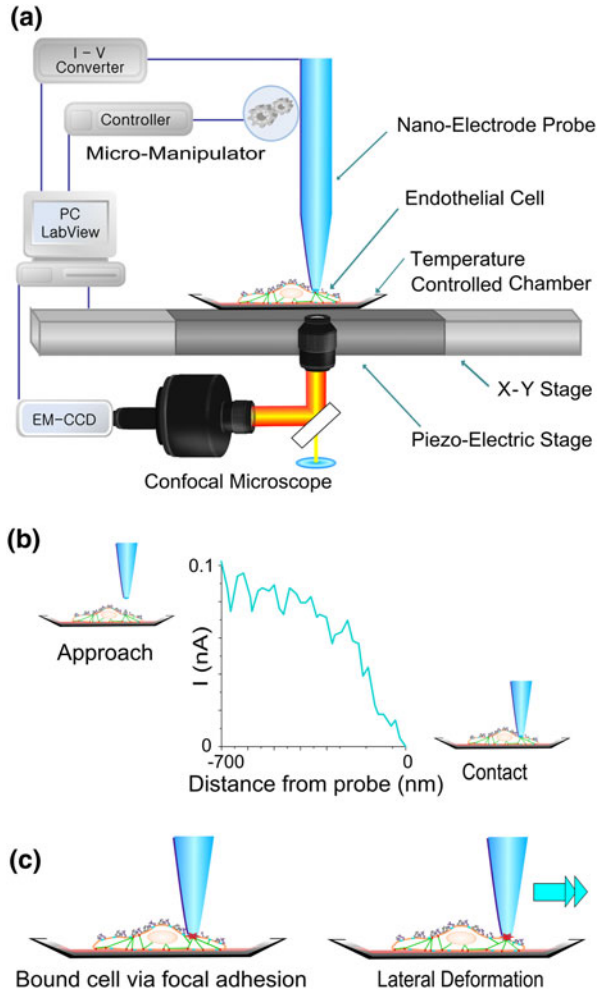

FIGURE 2. Experimental setup and procedure. (a) Experimental instrumentation enables precise timing of probe-cell contact *via* a nanoelectrode probe positioning system consisting of a nanoelectrode, piezoelectric stage, and a confocal microscope. (b) Probe-cell contact timing is obtained by noting the current drop of the nanoelectrode as it approaches the cell. (c) Experimental procedure: left: functionalized probe-cell contact and binding; right: subsequent manipulation of the FA by the probes on the apical surface of the cell.

International, Sunderland, UK) coupled to an EMCCD digital imaging camera (Sensicam-EM; Cooke Corporation, Romulus, MI, USA).

The nanoelectrode probe was functionalized with FN as previously described[23] and was mounted on a computer-controlled micromanipulator (MP-285; Sutter Instruments, Novato, CA, USA). A patch clamp amplifier (Model 2400, A-M Systems, Inc., Carlsborg, WA, USA) connected to a 20 MΩ probe detected current changes through the nanoelectrode. Together with a multifunction data acquisition board (NI PCI 6229, National Instruments, Austin, TX, USA) and LabVIEW software, the system coordinated nanoelectrode positional feedback control of the micro-manipulator and piezoelectric stage position using electrode current as the feedback process variable.

Induction and Manipulation of Focal Adhesions Using Functionalized Electrodes

Functionalized nanoelectrode probes were brought near the cell using the piezoelectric stage, while monitoring the current between the tip and the cell (Fig. 2b). After contact, the FN-coated probe was allowed to bind to the cell for 15 min at a location approximately halfway between the nucleus and the outer edge in order to later capture the membrane raft response of the majority of the apical plane. FA deformation (Fig. 2c) was accomplished by displacing the adhered probe parallel to the apical cell membrane by 1 μm. The probe was displaced in the positive x direction which corresponded to a FA translocation away from the nucleus approximately perpendicular to either the major or minor axis of the cell. In order to measure the time course of molecular scale activation in newly formed FAs, the FN-functionalized probe was allowed to come into contact with BAECs transfected with RFP-talin. Where indicated, compiled data is represented as mean ± standard deviation with $n \geq 3$ (different cells from different cultures). Statistical significance was evaluated using a Student's t test at the $p < 0.05$ level.

Tracking of Membrane Rafts and Kinetic Assays of GM1 and Talin Accumulation

Real time locations of membrane rafts were individually mapped using ImageJ tracking functions. In the case of passive displacement and active recoil, individual raft locations were manually tracked one at a time and frame-by-frame using the "Manual Tracking" plugin. For control cells the "Spot Tracker 2D" plugin was used with a 3 pixel square size for centering. For GM1 and talin kinetics, regions of interest from time-lapsed images were quantified and the fluorescence reduction values were added back to values assessed near the electrode adhesion point. The resulting values were then normalized by initial intensity and plotted with respect to time.

RESULTS

Rafts Passively Displace in Response to FA Deformation

Individual apical raft trajectories were tracked during FA deformation and while deformation was maintained (Fig. 3a). Displacements from multiple cells were

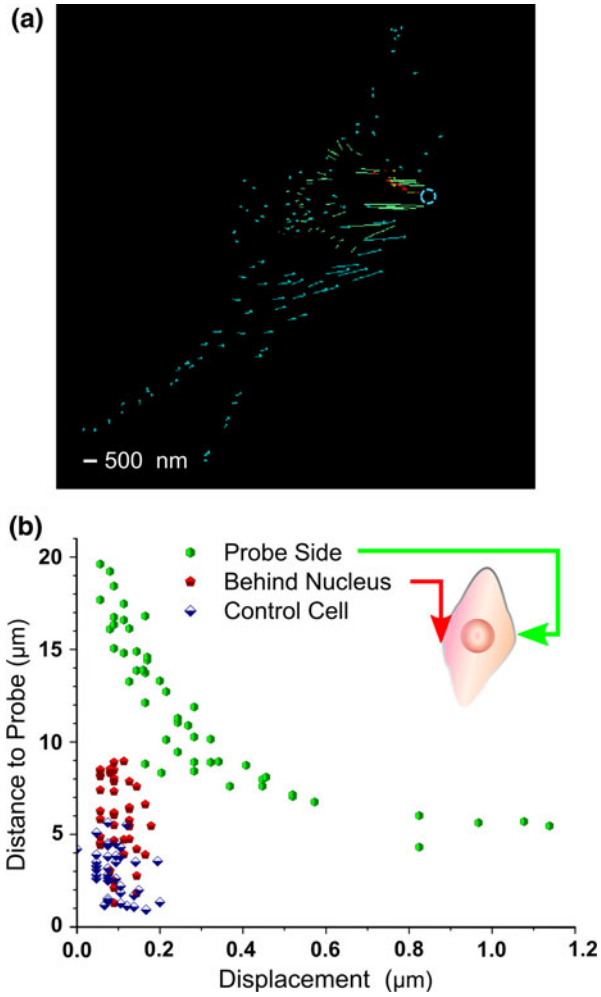

FIGURE 3. Passive membrane raft response. (a) Rafts from multiple cells were tracked and overlaid to create a composite image of raft trajectories (n = 4 cells), in response to a 1 μm displacement of a FA. The probe (circle) was displaced in the positive x direction which corresponds to a FA translocation away from the nucleus approximately perpendicular to the main axis of the cell. The probe was initially located approximately halfway between the nucleus and the outer edge of the cell. Individual trajectories initiated at the point furthest from the probe location (circle) and terminate closer to the probe. (b) Distance to probe vs. displacement magnitude of individual rafts. Green group (hexagons) corresponds to rafts that are located on the same side as the probe (relative to the nucleus); the red group (pentagons) corresponds to rafts located behind the nucleus (relative to the probe); control rafts are in blue (diamonds).

normalized by assigning the origin to the probe site and plotting raft locations relative to the probe site. Raft locations and displacements were then plotted on a common figure (Fig. 3a) and analyzed together (Fig. 3b). First, rafts simultaneously displaced in response to FA displacement. This simultaneous response occurred not only in rafts located near the probe-cell contact point but also in remote rafts. Figure 3b depicts responses of individual rafts as a function of their distance from the probe vs. their passive displacement magnitude. This passive response could be divided into two subpopulations, rafts that were located between the probe and nucleus and rafts located on the opposite side of the nucleus. Rafts that were on the same side of the nucleus as the probe displaced with magnitudes which decreased as the distance between the membrane raft and the location of the probe increased [green group (hexagons)]. Displacements of rafts that were located on the opposite side of the nucleus [red group (pentagons)] were nearly identical to displacements of rafts from control cells in which no FA displacement was induced [blue group (diamonds)].

Rafts Recoil After FA Deformation and Passive Raft Displacement

Subsequent to FA displacement the probe was maintained in its position and cells were imaged over time using confocal microscopy in order to capture the response of apical membrane rafts. Within the first minute after deformation a small subpopulation of rafts exhibited displacement in the opposite direction of the displacement applied by the probe, indicating raft recoil (Fig. 4a). The trajectories are plotted from the raft location closer to the probe location and terminate where the raft finished its motion. The subsequent remodeling is indicated by the overlapped tracked displacements resulting in a clustered trajectory endpoint. The magnitude of the recoil was greater for rafts that were closer to the probe, and smaller for more remote locations (Fig. 4b). 21% of all rafts exhibited recoil. However, considering that the location of all active rafts that recoiled coincided spatially with the probe side of the cell (relative to the nucleus) out of the population of rafts located on the probe side, 38% exhibited active recoil.

Directions of Passive Response and Active Recoil Coincided with FA Deformation Direction

We defined the displacement of the probe as the positive x-direction, for which 0 degrees was assigned as a reference direction, meaning that any deformation that is aligned with the direction of probe displacement would be aligned to the 0 degree mark. The raft displacement angles relative to the horizontal (0°) were calculated and used to determine directionality as functions of magnitude of displacement and distance from the probe. Figure 5 contains these directionality plots and illustrates the angle of individual raft displacements with respect to the horizontal in degrees, the magnitude of displacement (as indicated by concentric circles), and distance from the probe (as mapped out by color gradients in each area). Local passive

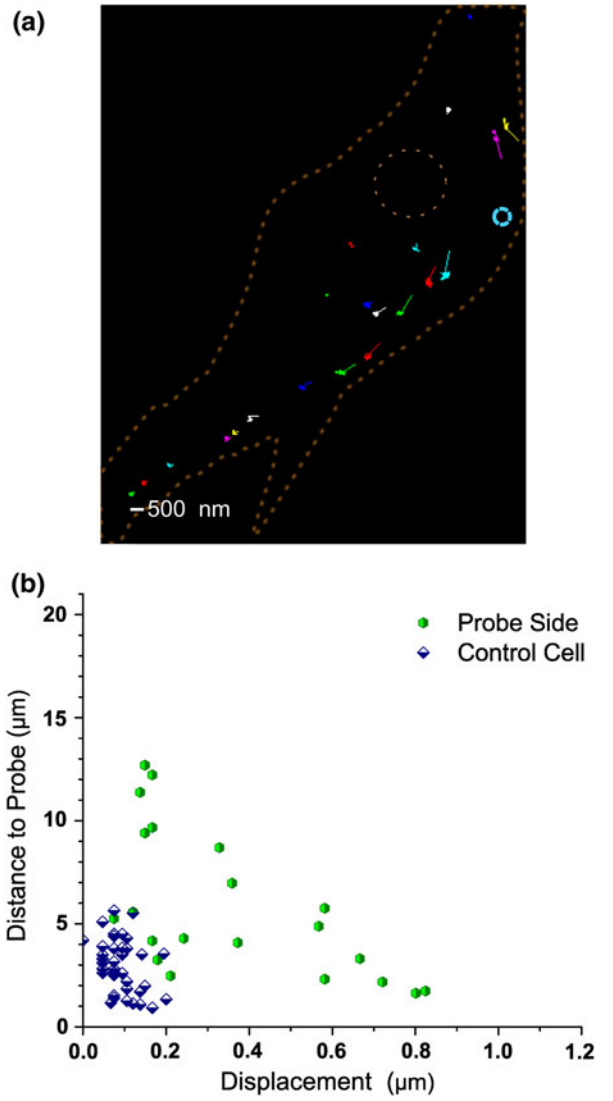

FIGURE 4. Active response: Recoil. (a) After deformation the probe was stationary and membrane rafts moved in the direction opposite to deformation, indicative of active recoil. Individual trajectories initiated closer to the probe location and terminate with subsequent continued remodeling as indicated by the overlapped tracked displacements resulting in a clustered trajectory endpoint. (b) Distance to probe vs. displacement of individual active rafts is plotted with the green group (pentagons) corresponding to rafts that are located on the same side as the probe (relative to the nucleus), and control rafts in blue (diamonds).

response of rafts was closely aligned with the direction of the applied FA displacement as demonstrated by the small angles ranging from 0 up to 30°, include the entire range of displacements from 0 to 1 μm, and are populated by local rafts up to 12.5 μm away (Fig. 5a). In addition, the local passive raft response aligned predominantly with the direction of FA displacement.

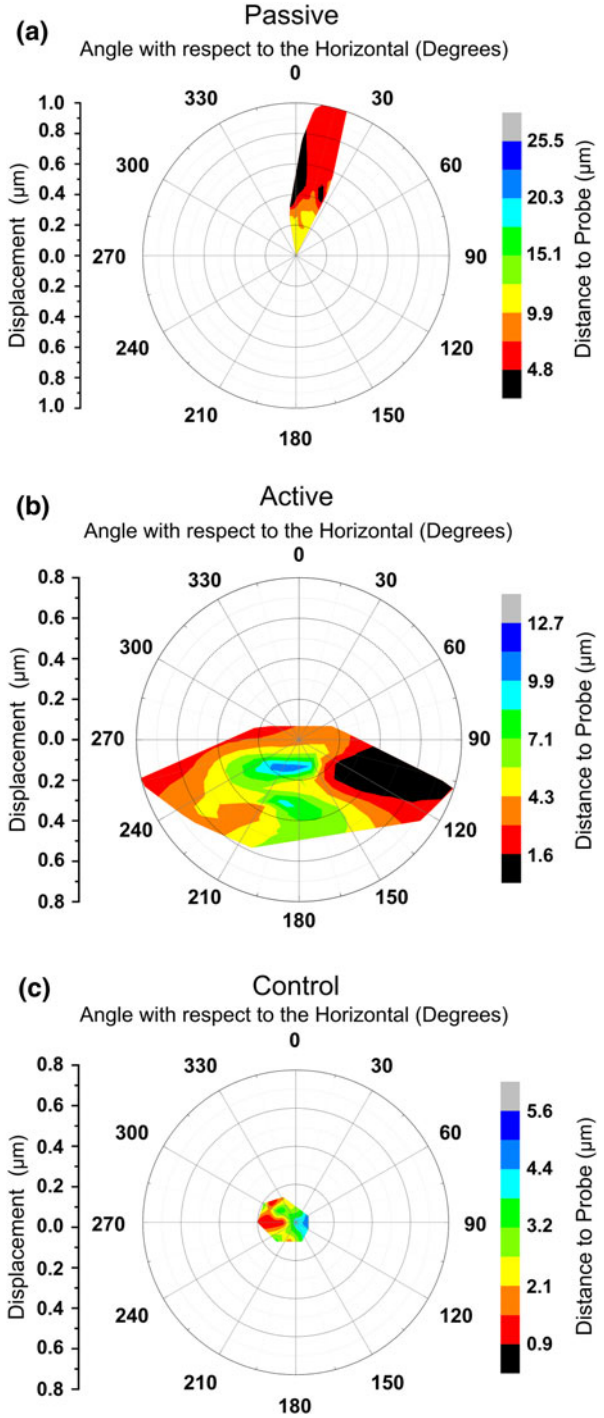

FIGURE 5. Directional dependence of passive and active membrane raft response. (a) Passive response aligned with the direction of FA displacement (aligned with 0°). (b) Active response was in the opposite direction of displacement ranging from angles between 90° and 270°, and covering a range of displacements up to 0.8 μm. (c) Control rafts do not exhibit a particular directionality as their displacements cover the full 360° range, and their magnitudes of displacement are less than 0.2 μm.

In contrast, rafts recoiled in the opposite direction of the FA displacement, as can be seen by the majority of responses exhibiting angles greater than 90° and less than 270° (Fig. 5b). The magnitudes of recoil range from 0.1 to 0.8 μm and occurred over a distance of 1.6 to 12.7 μm from the probe with an average ratio of passive displacement to active recoil of 1.06 ± 0.05. Both the active and the passive responses were different than rafts in control cells (Fig. 5c) where the magnitudes of displacements were less than 200 nm. Rafts in control cells (probe-cell contact without deformation) did not exhibit directionality of movement, and their angles relative to the horizontal were spread throughout the full 360° range. Thus, membrane rafts sensed FA translocation by passively displacing toward the probe, and actively recoiled in a direction away from the probe. In addition, the magnitude of passive and active responses was greater the closer the rafts were to the site of FA deformation.

Rafts and Talin Rapidly and Sequentially Accumulate at New Focal Adhesions

The FN-functionalized electrode probe contacted the apical cell surface with the $t = 0$ time point defined by a 2% drop of current through the electrode[17] (final portion of current drop is shown in Fig. 2b). After contact, a rapid increase in GM1 accumulation occurred around the probe site followed by accumulation of talin (Fig. 6a). Within the first 5 s after contact, GM1 fluorescence rapidly increased and reached a plateau at 10 s (Fig. 6a, green group) that was 14 ± 4.6% greater than control (Fig. 6b, left). The control group assayed the GM1 intensities on the apical membrane in absence of probe cell contact. All intensities were normalized relative to their initial intensity. The characteristic time constant of GM1 increase was 1.7 s, as calculated using an exponential recovery fitting model (not shown). In addition, rapid accumulation of GM1 coincided with the probe location and the surrounding area as illustrated in Fig. 6c. Kinetics of transfected RFP-talin accumulation after probe-cell contact was also assayed. Initially, talin did not increase near the probe (Fig. 6a). After 20 s, however, talin accumulated rapidly with a characteristic time constant of 0.57 ± 0.13 s and reached a plateau at 30 s with an increase of 2.26 ± 1.14 fold (Fig. 6b).

Rafts and Talin Rapidly and Sequentially Accumulate After Focal Adhesion Deformation

Upon 1 μm apical FAs deformation, GM1 accumulated by 15 ± 3.8% within 5 s around the probe site followed by accumulation of talin (Fig. 7b). Increase in

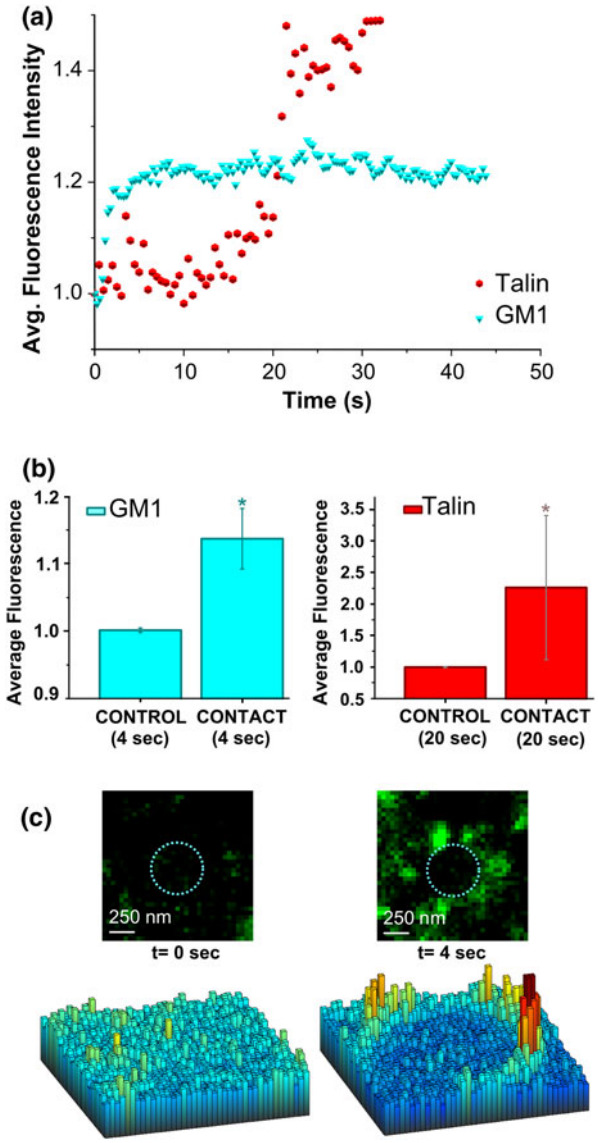

FIGURE 6. Kinetic response of membrane rafts and talin upon contact. (a) GM1 fluorescence accumulated with a time constant of 1.68 s, reached a plateau at 10 s. This increase was followed by accumulation of talin at 20 s that reached a plateau at 30 s. (b) On average, GM1 accumulation increased 14 ± 4.6% whereas talin increased by 2.26 ± 1.14% (n = 3). (c) (Top) GM1 accumulation around the probe (circle) is represented by 3-D intensity maps (Bottom).

accumulation was measured relative to the control samples which assayed accumulation prior to deformation. The characteristic time constant of GM1 response upon deformation was 0.3 s, as calculated by fitting an exponential recovery model to data in Fig. 7a (not shown). After the displacement neither the probe nor the cell were moved, and fluorescence was measured continually during the first minute. After 6 s, talin begins rapid accumulation reaching a 11 ± 3.1% increase with a characteristic time constant of 0.16 ± 0.04 s. Thus, GM1 accumulation occurred

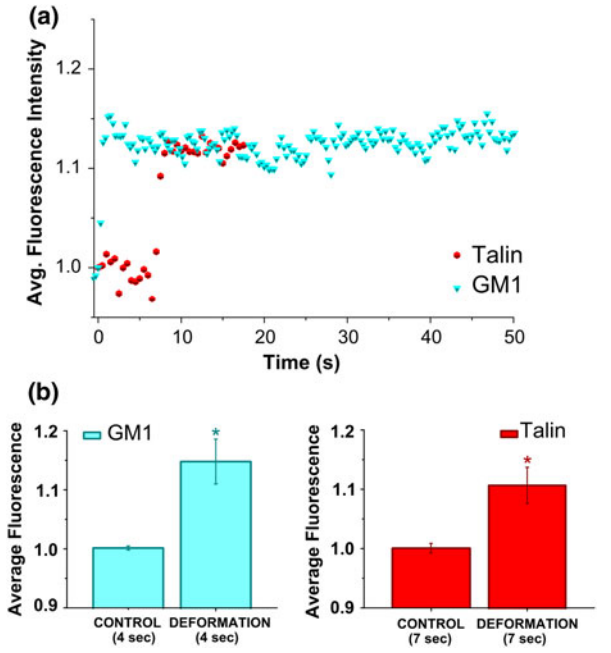

FIGURE 7. Kinetic response of membrane rafts and talin upon deformation. (a) Upon FA-deformation, GM1 accumulated with a characteristic time constant of 0.3 s and reached a plateau at 3 s followed by accumulation of talin at 7 s reaching a plateau at 10 s. (b) GM1 accumulation increased 15 ± 3.8% whereas talin increased by 11 ± 3.1% (n = 3).

within milliseconds after FA deformation followed later by talin accumulation.

Deformation Induces Long Term Accumulation of Membrane Rafts that is Reversible

Over tens of minutes after deformation, GM1 accumulation occurred first around the probe site (t = 163, 357, and 1419 s) and continued to increase radially away from the probe (t = 2288 s; Fig. 8a). The region of interest (indicated in the t = 2288 time point in Fig. 8a) was analyzed for fluorescence intensity from t = 0 to t = 2288 s. GM1 continuously and monotonically increased after deformation in and around the probe site (Fig. 8b and insets). On average, GM1 increased by 7.9 ± 1.6% from the 10 to 15 min time points (Fig. 8c) relative to control raft intensities prior to deformation. After maintaining FA deformation for about 30 min, the nanoelectrode probe was brought back to its initial position. Removal of deformation was accompanied by a decrease of GM1 fluorescence (Fig. 9a) that was radially dependent (insets), and leveled off after 10 min. Average decrease in accumulation upon reversal was 41.4 ± 7.4% (Fig. 9b) relative to control GM1 intensity prior to reversal.

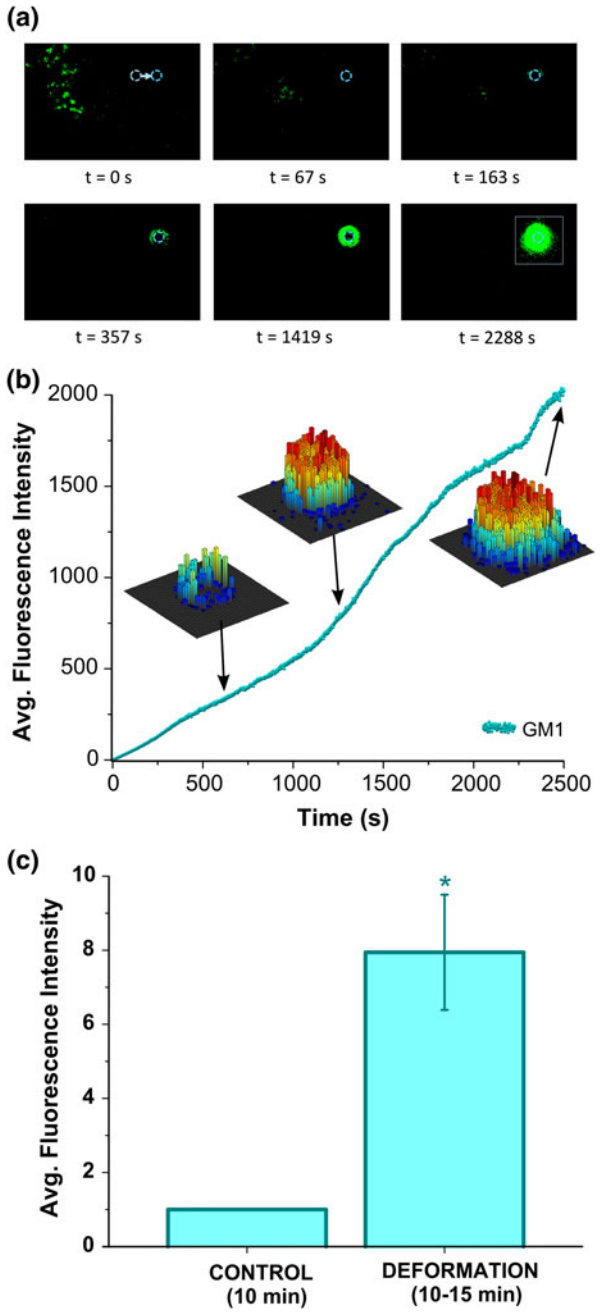

FIGURE 8. Deformation induces long term accumulation of membrane rafts. (a) Selected frames of time-lapsed images of GM1 display six time points starting at t = 0 with initial and final locations of the probe (circles). GM1 accumulation continued to increase first around the probe site (t = 163, 357, and 1419 s) and continued to grow radially outward (away from the probe) and inward (inside the probe). (b) Long term kinetic response of GM1 accumulation exhibited a continuous increase; insets represent 3-D displaying of intensity and radial geometry of accumulation. (c) An average increase of 7.9 ± 1.6% (n = 3) in intensity from the initial value was observed at time points ranging from 10 to 15 min after deformation.

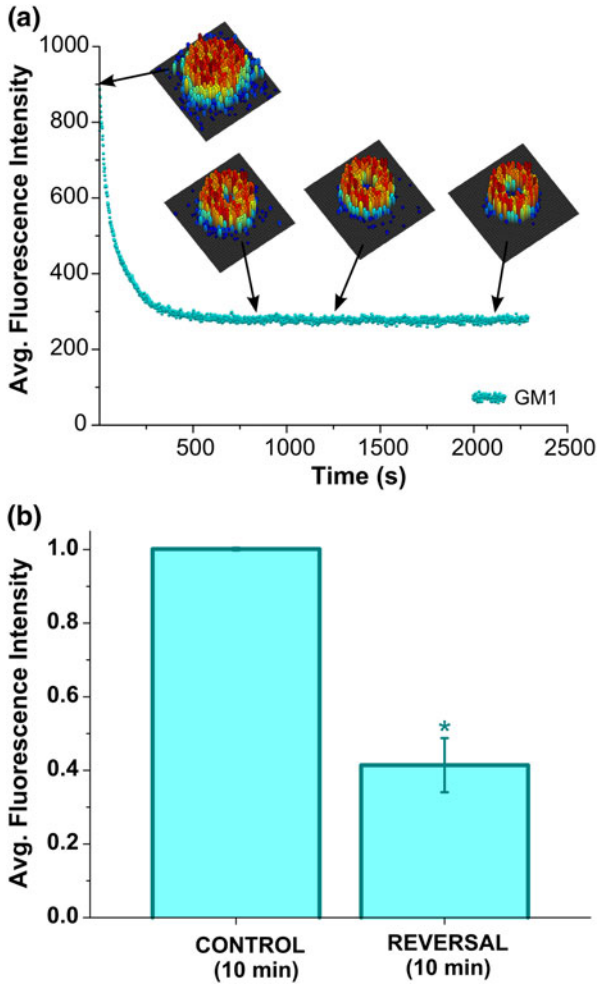

FIGURE 9. GM1 fluorescence decreases upon reversal of deformation. (a) Reversal of GM1 accumulation was continuous and leveled off after 10 min. The radial decrease is depicted by the insets showing 3-D representation of GM1 fluorescence intensity around the probe site. (b) Average decrease in accumulation upon reversal was 41.4 ± 7.4% (n = 3).

DISCUSSION

The main findings of this study are that non-mobile rafts displace passively in response to FA deformation with magnitudes that decrease with increasing distance from the FA. Displaced rafts actively recoil back to their original positions, particularly for those rafts that exhibited initial larger displacements. For the region of the cell located behind the nucleus (relative to the probe location), the nucleus appears to prevent raft displacements. The mobile subset of rafts (also labeled by cholera toxin) rapidly accumulates after FN has made contact with the cell, increases in accumulation upon FA deformation, continues to increase over 30 min of sustained deformation, and disperses when deformation is released. With respect to short time kinetics, rafts respond immediately to adhesion and deformation, while talin accumulates on the order of tens of seconds later. Thus mobile rafts participate in FA formation and reinforcement at very early times and prior to talin accumulation.

Mechanical Coupling from Focal Adhesions to Local and Remote Rafts

The observation that FA mechanical manipulation induces directional passive deformation of lipid rafts suggests that there is mechanical coupling between FAs and rafts. Potential sources of this mechanical coupling include the plasma membrane spectrin (fodrin) submembranous cytoskeleton, and the internal cytoskeleton composed of actin, microtubules, and intermediate filaments. It has been previously reported that lipid modifications such as glycosylphosphatidylinositol (GPI) anchors, palmitoylation, or myristoylation can target proteins to lipid rafts.[40,62] In turn, GPI-anchored proteins, as well as integrins, are associated with the cytoskeleton.[27,64,66] In addition, cytoskeletal components are linked to membrane rafts[3,20,27,29,47,49,57,63,64] and membrane rafts may be necessary for the coupling of the membrane to the cytoskeleton[42] as manipulation of membrane cholesterol content alters cytoskeleton-raft association. It is also known that when association of ezrin (which interacts with actin filaments *via* actin binding sites) with lipid rafts was decreased, the ability of lipid rafts to coalescence into larger signaling platforms was enhanced[27,29] suggesting that rafts were freed from their cytoskeletal constraints. These indications that rafts are anchored are consistent with a hypothesis that rafts can mechanosense locally and remotely through their connection to the cytoskeleton. The fact that raft displacement decreased with increasing distance from the displaced FA suggests that this displacement was passive, much like the passive deformation of remote points to a point displacement in a large elastic sheet (results from finite element simulation, not shown). Additionally, the lack of displacement of rafts on the side of the nucleus opposite the displaced FA is consistent with passive deformation that would be expected if the nucleus was considerably stiffer than the rest of the cytoplasm.[19] In summary, a subpopulation of anchored rafts responds locally and remotely with directional and spatial dependence to deformation of a FA. This mechanosensation is similar to other modes of cytoskeleton-linked mechanosensation which occurs at long distances from the point of applied force.[33–35,39,69,70]

A subset of membrane rafts recoiled within minutes after initial passive deformation. This recoil was in the direction away from the probe and was greatest for

those rafts that experienced the greatest initial deformation. Furthermore, Fig. 4a illustrates raft recoil in a representative cell with a general orientation along the major axis of the cell and in a direction opposite to probe displacement. This behavior was evident regardless of whether the probe was pulled in a direction along the major or minor axis of the cell. Recoil of rafts was also observed to be parallel to the direction of displacement but in the opposite direction. One possible explanation for this phenomenon is that initial deformation worked against the action of a molecular motor clutch, such as an isoform of myosin, that was bound to the raft and cytoskeleton, and altered the directionality of the complex, resulting in motor activity being oriented in the direction opposite to the passive deformation.[10,12,17,25,32,43,52] Previous studies have shown that resistance of the cell to pulling of the apical membrane using an optical trap may be due to the involvement of Src family kinases (SFK) in that SFK activation is vital for the FN rigidity sensing process.[38,68] However, we cannot discount the possibility that the recoil was passive and resulted from the detachment of a spring-like mechanism. Interestingly, however, active cellular recoil has also been previously reported to occur within seconds in response to applied stress[11] by a myosin-dependent mechanism, suggesting that mechanisms of active recoil in response to mechanical stress exist in cells.

Dynamic Kinetic Response: Mobility of Membrane Rafts

Adhesion led to immediate recruitment of mobile membrane rafts. This coalescence occurred in the absence of force application and preceded the recruitment of talin, suggesting that recruitment of rafts occurs prior to the activation of integrins. Upon adhesion, membrane rafts are known to be involved in the aggregation of integrins,[24,28,51,53,66] and upon integrin-mediated detachment, rafts internalize or dissolve.[14,15,28,67] Upon detachment, the cell also triggers the release of phosphorylated caveolin from FAs, which in turn permits its association with caveolae in order to induce the endocytosis of lipid rafts.[9] Other studies have also observed that when cells detach, integrin-mediated processes lead to the internalization and dissociation of lipid rafts.[53] We propose, therefore, that rafts participate in the reinforcement of FAs after initial integrin ligation by coalescing additional integrins leading to increased integrin avidity. This coalescence of integrins allows the additional integrins to undergo activation and the cells to firmly adhere. In a previous study, we found that contact time needed to be sustained for at least 5 min[22] suggesting that firm adhesion depended on the kinetics of integrin accumulation, which may be a diffusion-limited process.[35] The observation that rafts accumulate before talin supports this hypothesis. However, it remains to be determined whether integrin activation leads to raft coalescence or whether raft coalescence occurs first. However, raft coalescence increased with applied force suggesting that the membrane, with the integrated participation of lipid and integrin components, is an early mechanosensor.

Indications for the coalescence of rafts also come both from studies in model membranes as well as live cell studies.[44,45] As the diffusion of membrane rafts are inhibited by initial integrin ligation by FN, the membrane becomes more inhomogeneous leading to diffusion of lipids and GPI-anchored proteins down concentration gradients, which in turn focuses membrane constituents leading to enhanced bioactivity.[45] Essentially, the dissociation and association of rafts in response to contact, deformation, and reversal of deformation, indicate that rafts are responsive to force within seconds and over tens of minutes. This kinetic spatial and temporal dependence of membrane raft mechanosensation demonstrates that the plasma membrane is involved in the formation and reinforcement of FAs in response to force.

We further report that rafts increased in concentration in and around the FA upon deformation. This increase occurred with a time constant of 0.3 s and continued over tens of minutes as deformation was held constant. In addition, rafts dispersed after the deformation was released but adhesion was maintained. These results suggest that rafts participate in FA reinforcement upon force application. While raft association with FAs has been documented, there do not appear to be any reports that rafts participate in FA reinforcement upon force application. Currently the mechanism of this reinforcement remains unclear. While it is possible that the commonly implicated players in FA reinforcement, Rho, Rac, and actin, may play a role, these intracellular proteins generally are not thought to appear until minutes after force application.[28] The time constant of 0.3 s for initial raft recruitment after force suggests that this phenomenon is one of the earliest reported and is comparable to the time constants for force-dependent ion channel activation.[48] We propose that raft mobility and coalescence is a necessary component of FA reinforcement upon force application and provides an additional mechanism of force sensing by cells.

SUMMARY

In summary, we provide evidence that membrane rafts participate in FA development at sites of

extracellular matrix–integrin attachment and that rafts respond to mechanical deformation of FAs. Relatively non-mobile raft response was both passive and active and occurred in a spatially and directionally dependent manner. Highly mobile subpopulations of membrane rafts reversibly accumulated at the probe site in response to adhesion and deformation. Furthermore, GM1 accumulated significantly earlier than talin both upon contact and upon deformation. In conclusion, we have demonstrated direct mechanosensation of membrane rafts to mechanical perturbation of FAs thus opening up a new avenue of investigation of mechanotransduction that focuses on force induced raft mobility and raft-dependent signaling.

ACKNOWLEDGMENT

This work was supported by grants to PJB from NIH (R01 HL 07754201) and NSF (BES 0238910).

REFERENCES

[1]Anthis, N. J., K. L. Wegener, F. Ye, C. Kim, B. T. Goult, E. D. Lowe, I. Vakonakis, N. Bate, D. R. Critchley, M. H. Ginsberg, and I. D. Campbell. The structure of an integrin/talin complex reveals the basis of inside-out signal transduction. *EMBO J*. 28:3623–3632, 2009.

[2]Askari, J. A., P. A. Buckley, A. P. Mould, and M. J. Humphries. Linking integrin conformation to function. *J. Cell. Sci*. 122:165–170, 2009.

[3]Bini, L., S. Pacini, S. Liberatori, S. Valensin, M. Pellegrini, R. Raggiaschi, V. Pallini, and C. T. Baldari. Extensive temporally regulated reorganization of the lipid raft proteome following T-cell antigen receptor triggering. *Biochem. J*. 369:301–309, 2003.

[4]Bouaouina, M., Y. Lad, and D. A. Calderwood. The N-terminal domains of talin cooperate with the phosphotyrosine binding-like domain to activate beta1 and beta3 integrins. *J. Biol. Chem*. 283:6118–6125, 2008.

[5]Brown, D. A., and E. London. Structure and function of sphingolipid- and cholesterol-rich membrane rafts. *J. Biol. Chem*. 275:17221–17224, 2000.

[6]Butler, P., and Y. Wang. Editorial note: molecular imaging and mechanobiology. *Cell. Mol. Bioeng*. 4:123–124, 2011.

[7]Calderwood, D. A. Integrin activation. *J. Cell. Sci*. 117: 657–666, 2004.

[8]Campbell, I. D., and M. H. Ginsberg. The talin–tail interaction places integrin activation on FERM ground. *Trends Biochem. Sci*. 29:429–435, 2004.

[9]Caswell, P. T., S. Vadrevu, and J. C. Norman. Integrins: masters and slaves of endocytic transport. *Nat. Rev. Mol. Cell Biol*. 10:843–853, 2009.

[10]Chan, C. E., and D. J. Odde. Traction dynamics of filopodia on compliant substrates. *Science* 322:1687–1691, 2008.

[11]Coughlin, M. F., D. D. Sohn, and G. W. Schmid-Schonbein. Recoil and stiffening by adherent leukocytes in response to fluid shear. *Biophys. J*. 94:1046–1051, 2008.

[12]Cross, R. A. Myosin's mechanical ratchet. *Proc. Natl Acad. Sci. USA* 103:8911–8912, 2006.

[13]Crossthwaite, A. J., T. Seebacher, N. Masada, A. Ciruela, K. Dufraux, J. E. Schultz, and D. M. Cooper. The cytosolic domains of Ca^{2+}-sensitive adenylyl cyclases dictate their targeting to plasma membrane lipid rafts. *J. Biol. Chem*. 280:6380–6391, 2005.

[14]del Pozo, M. A., N. B. Alderson, W. B. Kiosses, H. H. Chiang, R. G. Anderson, and M. A. Schwartz. Integrins regulate Rac targeting by internalization of membrane domains. *Science* 303:839–842, 2004.

[15]del Pozo, M. A., N. Balasubramanian, N. B. Alderson, W. B. Kiosses, A. Grande-Garcia, R. G. Anderson, and M. A. Schwartz. Phospho-caveolin-1 mediates integrin-regulated membrane domain internalization. *Nat. Cell Biol*. 7:901–908, 2005.

[16]del Pozo, M. A., and M. A. Schwartz. Rac, membrane heterogeneity, caveolin and regulation of growth by integrins. *Trends Cell Biol*. 17:246–250, 2007.

[17]DoHarris, L., A. Giesler, B. Humber, A. Sukumar, and L. J. Janssen. Molecular motors: how to make models that can be used to convey the concept of molecular ratchets and thermal capture. *Adv. Physiol. Educ*. 35:213–218, 2011.

[18]Eggeling, C., C. Ringemann, R. Medda, G. Schwarzmann, K. Sandhoff, S. Polyakova, V. N. Belov, B. Hein, C. von Middendorff, A. Schonle, and S. W. Hell. Direct observation of the nanoscale dynamics of membrane lipids in a living cell. *Nature* 457:1159–1162, 2009.

[19]Ferko, M. C., A. Bhatnagar, M. B. Garcia, and P. J. Butler. Finite-element stress analysis of a multicomponent model of sheared and focally-adhered endothelial cells. *Ann. Biomed. Eng*. 35:208–223, 2007.

[20]Foster, L. J., C. L. De Hoog, and M. Mann. Unbiased quantitative proteomics of lipid rafts reveals high specificity for signaling factors. *Proc. Natl Acad. Sci. USA* 100:5813–5818, 2003.

[21]Frame, M. D., R. J. Rivers, O. Altland, and S. Cameron. Mechanisms initiating integrin-stimulated flow recruitment in arteriolar networks. *J. Appl. Physiol*. 102:2279–2287, 2007.

[22]Fuentes, D. E., C. B. Bae, and P. J. Butler. Focal adhesion induction at the tip of a functionalized nanoelectrode. *Cell. Mol. Bioeng*. 4:616–626, 2011.

[23]Fullekrug, J., and K. Simons. Lipid rafts and apical membrane traffic. *Ann. N. Y. Acad. Sci*. 1014:164–169, 2004.

[24]Gaus, K., L. S. Le, N. Balasubramanian, and M. A. Schwartz. Integrin-mediated adhesion regulates membrane order. *J. Cell Biol*. 174:725–734, 2006.

[25]Gebhardt, J. C., A. E. Clemen, J. Jaud, and M. Rief. Myosin-V is a mechanical ratchet. *Proc. Natl Acad. Sci. USA* 103:8680–8685, 2006.

[26]Gomez-Mouton, C., J. L. Abad, E. Mira, R. A. Lacalle, E. Gallardo, and S. Jimenez-Baranda. Segregation of leading-edge and uropod components into specific lipid rafts during T cell polarization. *Proc. Natl. Acad. Sci. USA* 98:9642–9647, 2001.

[27]Goswami, D., K. Gowrishankar, S. Bilgrami, S. Ghosh, R. Raghupathy, R. Chadda, R. Vishwakarma, M. Rao, and S. Mayor. Nanoclusters of GPI-anchored proteins are formed by cortical actin-driven activity. *Cell* 135:1085–1097, 2008.

[28]Guan, J. L. Cell biology. Integrins, rafts, Rac, and Rho. *Science* 303:773–774, 2004.

[29]Gupta, N., B. Wollscheid, J. D. Watts, B. Scheer, R. Aebersold, and A. L. DeFranco. Quantitative proteomic analysis of B cell lipid rafts reveals that ezrin regulates

antigen receptor-mediated lipid raft dynamics. *Nat. Immunol.* 7:625–633, 2006.
[30]Harder, T., P. Scheiffele, P. Verkade, and K. Simons. Lipid domain structure of the plasma membrane revealed by patching of membrane components. *J. Cell Biol.* 141:929–942, 1998.
[31]Hein, T. W., S. H. Platts, K. R. Waitkus-Edwards, L. Kuo, S. A. Mousa, and G. A. Meininger. Integrin-binding peptides containing RGD produce coronary arteriolar dilation via cyclooxygenase activation. *Am. J. Physiol. Heart Circ. Physiol.* 281:H2378–H2384, 2001.
[32]Houdusse, A., and H. L. Sweeney. Myosin motors: missing structures and hidden springs. *Curr. Opin. Struct. Biol.* 11:182–194, 2001.
[33]Hu, S., J. Chen, B. Fabry, Y. Numaguchi, A. Gouldstone, D. E. Ingber, J. J. Fredberg, J. P. Butler, and N. Wang. Intracellular stress tomography reveals stress focusing and structural anisotropy in cytoskeleton of living cells. *Am. J. Physiol. Cell Physiol.* 285:C1082–C1090, 2003.
[34]Huang, H., R. D. Kamm, and R. T. Lee. Cell mechanics and mechanotransduction: pathways, probes, and physiology. *Am. J. Physiol. Cell Physiol.* 287:C1–C11, 2004.
[35]Ingber, D. E. Cellular mechanotransduction: putting all the pieces together again. *FASEB J.* 20:811–827, 2006.
[36]Jacobson, K., O. G. Mouritsen, and R. G. Anderson. Lipid rafts: at a crossroad between cell biology and physics. *Nat. Cell Biol.* 9:7–14, 2007.
[37]Jalali, S., M. A. del Pozo, K. Chen, H. Miao, Y. Li, M. A. Schwartz, J. Y. Shyy, and S. Chien. Integrin-mediated mechanotransduction requires its dynamic interaction with specific extracellular matrix (ECM) ligands. *Proc. Natl Acad. Sci. USA* 98:1042–1046, 2001.
[38]Jiang, G., A. H. Huang, Y. Cai, M. Tanase, and M. P. Sheetz. Rigidity sensing at the leading edge through alphavbeta3 integrins and RPTPalpha. *Biophys. J.* 90:1804–1809, 2006.
[39]Katsumi, A., A. W. Orr, E. Tzima, and M. A. Schwartz. Integrins in mechanotransduction. *J. Biol. Chem.* 279:12001–12004, 2004.
[40]Kniep, B., T. Cinek, P. Angelisova, and V. Horejsi. Association of the GPI-anchored leucocyte surface glycoproteins with ganglioside GM3. *Biochem. Biophys. Res. Commun.* 203:1069–1075, 1994.
[41]Kwik, J., S. Boyle, D. Fooksman, L. Margolis, M. P. Sheetz, and M. Edidin. Membrane cholesterol, lateral mobility, and the phosphatidylinositol 4,5-bisphosphate-dependent organization of cell actin. *Proc. Natl Acad. Sci. USA* 100:13964–13969, 2003.
[42]Levitan, I., and K. J. Gooch. Lipid rafts in membrane-cytoskeleton interactions and control of cellular biomechanics: actions of oxLDL. *Antioxid. Redox Signal.* 9:1519–1534, 2007.
[43]Lin, Y. Mechanics model for actin-based motility. *Phys. Rev. E. Stat. Nonlinear Soft Matter* 79(021916):2009, 2009.
[44]Lingwood, D., J. Ries, P. Schwille, and K. Simons. Plasma membranes are poised for activation of raft phase coalescence at physiological temperature. *Proc. Natl Acad. Sci. USA* 105:10005–10010, 2008.
[45]Lingwood, D., and K. Simons. Lipid rafts as a membrane-organizing principle. *Science* 327:46–50, 2010.
[46]Lu, S., M. Ouyang, J. Seong, J. Zhang, S. Chien, and Y. Wang. The spatiotemporal pattern of Src activation at lipid rafts revealed by diffusion-corrected FRET imaging. *PLoS Comput. Biol.* 4:e1000127, 2008.
[47]MacLellan, D. L., H. Steen, R. M. Adam, M. Garlick, D. Zurakowski, S. P. Gygi, M. R. Freeman, and K. R. Solomon. A quantitative proteomic analysis of growth factor-induced compositional changes in lipid rafts of human smooth muscle cells. *Proteomics* 5:4733–4742, 2005.
[48]Matthews, B. D., C. K. Thodeti, J. D. Tytell, A. Mammoto, D. R. Overby, and D. E. Ingber. Ultra-rapid activation of TRPV4 ion channels by mechanical forces applied to cell surface beta1 integrins. *Integr. Biol. (Camb.)* 2:435–442, 2010.
[49]McMahon, K. A., M. Zhu, S. W. Kwon, P. Liu, Y. Zhao, and R. G. Anderson. Detergent-free caveolae proteome suggests an interaction with ER and mitochondria. *Proteomics* 6:143–152, 2006.
[50]Merritt, E. A., S. Sarfaty, F. van den Akker, C. L'Hoir, J. A. Martial, and W. G. Hol. Crystal structure of cholera toxin B-pentamer bound to receptor GM1 pentasaccharide. *Protein Sci.* 3:166–175, 1994.
[51]Mitchell, J. S., W. S. Brown, D. G. Woodside, P. Vanderslice, and B. W. McIntyre. Clustering T-cell GM1 lipid rafts increases cellular resistance to shear on fibronectin through changes in integrin affinity and cytoskeletal dynamics. *Immunol. Cell Biol.* 87:324–336, 2009.
[52]Mogilner, A., and G. Oster. Force generation by actin polymerization II: the elastic ratchet and tethered filaments. *Biophys. J.* 84:1591–1605, 2003.
[53]Norambuena, A., and M. A. Schwartz. Effects of integrin-mediated cell adhesion on plasma membrane lipid raft components and signaling. *Mol. Biol. Cell* 22:3456–3464, 2011.
[54]Norman, L. L., R. J. Oetama, M. Dembo, F. Byfield, D. A. Hammer, I. Levitan, and H. Aranda-Espinoza. Modification of cellular cholesterol content affects traction force, adhesion and cell spreading. *Cell. Mol. Bioeng.* 3:151–162, 2010.
[55]Parton, R. G. Ultrastructural localization of gangliosides; GM1 is concentrated in caveolae. *J. Histochem. Cytochem.* 42:155–166, 1994.
[56]Pike, L. J. Rafts defined: a report on the Keystone symposium on lipid rafts and cell function. *J. Lipid Res.* 47:1597–1598, 2006.
[57]Pike, L. J. The challenge of lipid rafts. *J. Lipid Res.* 50(Suppl):S323–S328, 2009.
[58]Rotblat, B., L. Belanis, H. Liang, R. Haklai, G. Elad-Zefadia, J. F. Hancock, Y. Kloog, and S. J. Plowman. H-Ras nanocluster stability regulates the magnitude of MAPK signal output. *PLoS One* 5:e11991, 2010.
[59]Scheiffele, P., M. G. Roth, and K. Simons. Interaction of influenza virus haemagglutinin with sphingolipid-cholesterol membrane domains via its transmembrane domain. *EMBO J.* 16:5501–5508, 1997.
[60]Schuck, S., and K. Simons. Polarized sorting in epithelial cells: raft clustering and the biogenesis of the apical membrane. *J. Cell. Sci.* 117:5955–5964, 2004.
[61]Singh, R. D., D. L. Marks, E. L. Holicky, C. L. Wheatley, T. Kaptzan, S. B. Sato, T. Kobayashi, K. Ling, and R. E. Pagano. Gangliosides and beta1-integrin are required for caveolae and membrane domains. *Traffic* 11:348–360, 2010.
[62]Smotrys, J. E., and M. E. Linder. Palmitoylation of intracellular signaling proteins: regulation and function. *Annu. Rev. Biochem.* 73:559–587, 2004.
[63]Sprenger, R. R., D. Speijer, J. W. Back, C. G. De Koster, H. Pannekoek, and A. J. Horrevoets. Comparative proteomics of human endothelial cell caveolae and rafts using two-dimensional gel electrophoresis and mass spectrometry. *Electrophoresis* 25:156–172, 2004.
[64]Suzuki, K. G., T. K. Fujiwara, F. Sanematsu, R. Iino, M. Edidin, and A. Kusumi. GPI-anchored receptor clusters

transiently recruit Lyn and G alpha for temporary cluster immobilization and Lyn activation: single-molecule tracking study 1. *J. Cell Biol.* 177:717–730, 2007.

[65]Tabouillot, T., H. S. Muddana, and P. J. Butler. Endothelial cell membrane sensitivity to shear stress is lipid domain dependent. *Cell. Mol. Bioeng.* 4:169–181, 2011.

[66]van Zanten, T. S., A. Cambi, M. Koopman, B. Joosten, C. G. Figdor, and M. F. Garcia-Parajo. Hotspots of GPI-anchored proteins and integrin nanoclusters function as nucleation sites for cell adhesion. *Proc. Natl Acad. Sci. USA* 106:18557–18562, 2009.

[67]Vassilieva, E. V., K. Gerner-Smidt, A. I. Ivanov, and A. Nusrat. Lipid rafts mediate internalization of beta1-integrin in migrating intestinal epithelial cells. *Am. J. Physiol. Gastrointest. Liver Physiol.* 295:G965–G976, 2008.

[68]von Wichert, G., G. Jiang, A. Kostic, K. De Vos, J. Sap, and M. P. Sheetz. RPTP-alpha acts as a transducer of mechanical force on alphav/beta3-integrin-cytoskeleton linkages. *J. Cell Biol.* 161:143–153, 2003.

[69]Wang, N., J. P. Butler, and D. E. Ingber. Mechanotransduction across the cell surface and through the cytoskeleton. *Science* 260:1124–1127, 1993.

[70]Wang, N., J. D. Tytell, and D. E. Ingber. Mechanotransduction at a distance: mechanically coupling the extracellular matrix with the nucleus. *Nat. Rev. Mol. Cell Biol.* 10:75–82, 2009.

[71]Yamabhai, M., and R. G. Anderson. Second cysteine-rich region of epidermal growth factor receptor contains targeting information for caveolae/rafts. *J. Biol. Chem.* 277:24843–24846, 2002.

[72]Yang, B. H., and V. Rizzo. TNF-alpha potentiates protein-tyrosine nitration through activation of NADPH oxidase and eNOS localized in membrane rafts and caveolae of bovine aortic endothelial cells. *Am. J. Physiol. Heart Circ. Physiol.* 292:H954–H962, 2007.